JOURNAL OF SPACECRAFT AND ROCKETS
Vol. 43, No. 5, September–October 2006

Solar Polar Orbiter: A Solar Sail Technology Reference Study

Malcolm Macdonald* and Gareth W. Hughes†
University of Glasgow, Glasgow, Scotland G12 8QQ, United Kingdom
Colin R. McInnes‡
University of Strathclyde, Glasgow, Scotland G1 XXJ, United Kingdom
and
Aleksander Lyngvi,§ Peter Falkner,¶ and Alessandro Atzei**
ESA, 2200 AG Noordwijk, The Netherlands

An assessment is presented of a Solar Polar Orbiter mission as a Technology Reference Study. The goal is to focus the development of strategically important technologies of potential relevance to future science missions. The technology is solar sailing, and so the use of solar sail propulsion is, thus, defined a priori. The primary mission architecture utilizes maximum Soyuz Fregat 2-1b launch energy, deploying the sail shortly after Fregat separation. The 153 × 153 m square sail then spirals into a circular 0.48-astronomical-unit orbit, where the orbit inclination is raised to 90 deg with respect to the solar equator in just over 5 years. Both the solar sail and spacecraft technology requirements have been addressed. The sail requires advanced boom and new thin-film technology. The spacecraft requirements were found to be minimal because the spacecraft environment is relatively benign in comparison with other currently envisaged missions, such as the Solar Orbiter mission and BepiColombo.

Introduction

THE Science Payload and Advanced Concepts Office of ESA has introduced Technology Reference Studies (TRS) to focus the development of strategically important technologies of likely relevance to future science missions. This is accomplished through the study of technologically demanding and scientifically interesting missions, which are not part of the ESA science program. This paper discusses one such mission, the Solar Polar Orbiter (SPO). The TRS cover a wide range of mission profiles, with an even wider range of strategically important technologies. All TRS mission profiles are based on small satellites, with miniaturized highly integrated payload suites, launched on a Soyuz Fregat 2-1b.[1]

Science missions are technologically very challenging. It is important to define and prepare critical technologies far in advance, hence, ensuring that they are developed in a timely manner and that associated cost, risk, and feasibility of potential future mission concepts can be properly estimated. The TRS are set up to provide a set of realistic requirements for these technology developments far before specific science missions are proposed by the scientific community. Through their study, a set of detailed requirements for technology development activities can be determined. The TRS are a tool to focus technology development activities; they are not part of ESA's science mission program. A TRS is carefully selected to address a wide range of technologies that have to be applicable to many other scientific mission profiles.

Terrestrial observations of the sun are restricted to the ecliptic plane and within the solar limb, thus, restricting observations to within ±7.25 deg of the solar equator. Close solar measurements at all latitudes are necessary to achieve a global three-dimensional picture of solar features and processes. Observations directly over the solar poles are imperative to understanding the sun. Most previous missions to study the sun have been restricted to observations from within the ecliptic. The Ulysses spacecraft used a Jupiter gravity assist to pass over the solar poles, obtaining field and particle measurements but no images of the poles.[2] Furthermore, the Ulysses orbit is highly elliptical, with a pole revisit time of approximately 6 years. It is desired that future solar analysis be performed much closer to the sun, as well as from an out-of-ecliptic perspective. The solar orbiter mission scheduled for launch in October 2013 intends to deliver a science suite of order 180 kg to a maximum inclination of order 35 deg with respect to the solar equator and to a minimum solar approach radius of 0.22 astronomical unit (AU) using solar electric propulsion (SEP).[3] The inability of the solar orbiter mission to attain a solar polar orbit highlights the difficulty of such a goal with conventional propulsion. A 1998 study considered the use of solar sail technology to place a science payload into a solar polar orbit.[4] In Ref. 4 a 164-kg spacecraft, using a 6 $g \cdot m^{-2}$, 158 × 158 m solar sail and a cruise time of 4.6 years is defined. Within this prior study, the definition of solar sail technology requirements is imprecise due to the technology status of solar sail hardware at the time.

The primary objective of the mission presented in this paper is to deliver a spacecraft into an orbit at 90-deg inclination with respect to the solar equator, using a launch vehicle no larger than the Soyuz Fregat 2-1b. The spacecraft orbit should be phased such that once on-station it will remain near to the solar limb from a terrestrial perspective. The spacecraft should also be positioned on an orbit interior to Earth's.

This paper summarizes the output from the SPO TRS, allowing definition of key technology requirements for this class of solar sail mission. The SPO TRS draws some significantly different conclusions from similar previous studies, many of which are due to the fundamentally different methodologies utilized; these will be discussed within this paper. In particular, in this paper, the mission concept is developed with realistic orbit trajectory generation to the actual science orbit rather than some approximation of this orbit. The SPO spacecraft systems are fully defined within the technology

Received 3 March 2005; revision received 8 August 2005; accepted for publication 26 August 2005.

*Research Assistant, Department of Aerospace Engineering; currently AOCS Engineer, SciSys, Ltd., Bristol, England BS4 5SS, United Kingdom; malcolm.macdonald@scisys.co.uk.

†Research Assistant, Department of Aerospace Engineering.

‡Professor, Department of Mechanical Engineering; colin.mcinnes@strath.ac.uk. Member AIAA.

§Space Systems Engineer, Postbus 299, Science Payload and Advanced Concepts Office, European Space Research and Technology Center, Keplerlaan 1; alyngvi@rssd.esa.int.

¶Head of Planetary Exploration Studies Section, Postbus 299, Science Payload and Advanced Concepts Office, European Space Research and Technology Center, Keplerlaan 1.

**Space Systems Engineer, Postbus 299, Science Payload and Advanced Concepts Office, European Space Research and Technology Center, Keplerlaan 1.

limits of the mission time frame and with consideration of the limitations due to the use of solar sail propulsion, such as pointing accuracy due to sail flexing. The solar sail system and technology requirements are also fully defined. A full range of mission architectures have been investigated to ensure that an optimal reference mission is generated. Furthermore, the global effect of varying the solar close approach radius is considered for the first time through amalgamation of trajectory and spacecraft/sail systems into one complete analysis.

Top-Level Baseline Science Objectives

The many potential science objectives and goals of a SPO mission have previously been discussed in detail in Ref. 4. The purpose of this paper is to address the technology goals and requirements of such a mission, and as such, discussion of science goals is limited to top-level baseline objectives.

The solar wind, in addition to higher energy solar flare particles, can induce power line surges and radio interference on the Earth, as well as causing the well-known aurora borealis. Observations from Ulysses shows that the 11-year solar cycle minimum causes the solar wind speed at polar latitudes to almost double the equatorial value, from a speed of order 450 to 750 $\text{km} \cdot \text{s}^{-1}$. The solar wind also appears to have a different composition at the solar poles. A close solar polar orbiter would, thus, enable further investigation into the polar solar wind data obtained by Ulysses and likely to be obtained from the solar orbiter mission over a range of inclinations up to 35 deg. Furthermore, it is important that we can obtain an understanding of the relationship between solar wind velocity and the solar magnetic field geometry, with the best location to assess accurately the longitudinal structure of the magnetic field in the corona being from polar latitudes. Solar polar observations would also address the scale over which the corotation of coronal plasma with the sun is lost. Combined coronagraph data would, thus, allow the determination of three-dimensional structures and show the locations of streamers, rays, and plumes in the corona. Considerable fine structures, termed microstreams, were observed in high-speed flow from coronal holes at the poles by Ulysses. When the microstreams were related to polar plumes, supergranulation patterns and bright flares would be enabled by a spacecraft in a solar polar orbit.[4]

Mission Architecture

The mission is split into seven core phases, ranging from launch through to sail jettison and the beginning of the science mission and then on into a potential extension to the science mission. The longest mission phase is the transfer trajectory, which is provisionally scheduled as 5 years, although this will vary depending on the final selected sail characteristic acceleration. We define characteristic acceleration as the acceleration the sail actually provides at a solar distance of 1 AU, with the sail normal to the sun line. Following the arrival of the spacecraft at the solar polar orbit, the sail is jettisoned to allow the science operations phase to begin. The spacecraft attitude and orbit maintenance is from this point on performed using a hydrazine system, as will be discussed later. Science operations are provisionally scheduled for 2 years.

The target solar polar orbit is defined by the direction of the solar poles. Thus, the desired polar orbit is inclined at 82.75 deg with a right ascension of ascending node of 255.8 deg at J2000 (corresponding to the Julian day 2451545) with a drift rate of plus 0.014 deg/year, within a standard ecliptic plane reference frame. Analysis of sunspots has revealed that the direction of the solar poles is less well defined than just indicated[5]; however, we adopt these values as the target orbit. Spacecraft orbit phasing with respect to the Earth must be carefully considered. Science returns are maximized when the spacecraft is positioned near to the solar limb as seen from Earth, allowing observation of the corona along the sun–Earth line. Maintaining this alignment eliminates solar conjunctions and, hence, loss of telemetry. Thus, it is considered necessary that the spacecraft orbit is in resonance with Earth's orbit about the sun.

Potential target solar orbits are defined as a circular polar orbit with radius $N^{-2/3}$ AU for integer values of N, where N is the orbit resonance number. Figure 1 shows the Earth–sun–sail separation angle for $1 \leq N \leq 5$. It is seen that as the orbit resonance number

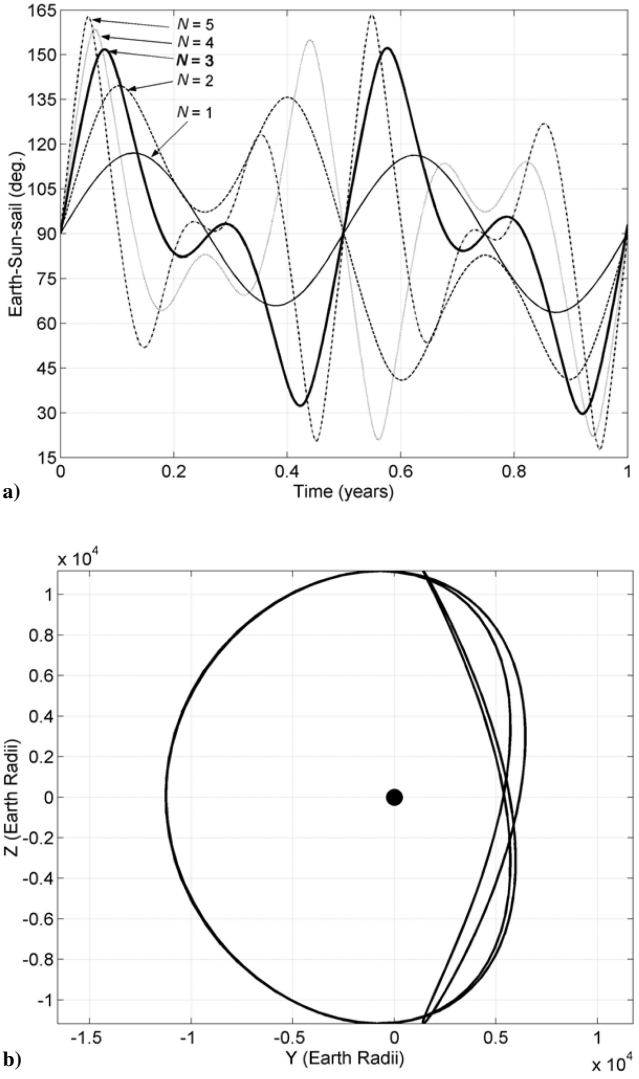

Fig. 1 SPO trajectory plot: a) Earth–sun–sail separation angle for $1 \leq N \leq 5$ and b) trajectory plot for $N = 3$ solar polar orbit in an Earth-centered rotating reference frame.

is increased, the separation angle tends farther from 90 deg, hence degrading mission science returns. At $N = 1$, the Earth–sun–sail separation angle stays within ± 27 deg of 90 deg, whereas at $N = 5$, the Earth–sun–sail separation angle peaks at over ± 73 deg from 90 deg. The choice of optimal resonant orbit depends on a number of factors. Far from the sun, larger aperture instruments are required to maintain image resolution, with only infrequent passes over the solar pole. However, the Earth–sun–sail separation angle stays close to 90 deg. Closer to the sun, we obtain frequent passes over the solar poles and very high-resolution imaging, but the spacecraft thermal environment becomes increasingly severe, while also passing farther from the solar limb. Thus, a balance must be sought based on spacecraft engineering constraints, cost, and science goals. The $N = 3$ resonant orbit is defined as the target scientific orbit because this places the spacecraft close to the sun, while also being in a relatively benign thermal environment compared to closer resonant orbits. This orbit also maintains the spacecraft within ± 30 deg of the solar limbs for the majority of the mission duration. Figure 1 also shows the trajectory of the solar polar orbit for $N = 3$. The trajectory is seen from an Earth-centered coordinate system, with the sun fixed along the negative X axis. The asymmetry for $N = 3$ (and $N = 1$) can be reversed by a simple alteration of the initial conditions.

Spacecraft Model

In this paper the term spacecraft means the vehicle that will perform the science operations at the defined target orbit and does not necessarily include the solar sail. Conventionally this craft has been

Table 1 Mass budget, with scaling laws rounded to one decimal place

System	CBE mass, kg	DMM, %	CBE mass plus DMM, kg
Science instruments	37.0	10.8	41.2
AOCS dry	28.7	5.0	30.1
TT&C	48.3	5.0	50.7
Onboard data handling (OBDH)	4.2	10.0	4.7
Thermal and Radiation	9.6	10.0	10.6
Power	42.9	8.3	46.8
Mechanisms and structure	49.2	7.5	53.0
Spacecraft nominal dry mass at launch			237.1
AOCS propellant, including sail separation allowance and a margin			10.8
Spacecraft nominal wet mass at launch			247.9
Solar sail nominal mass at launch[a]			195.9
Nominal launch mass			443.9
ESA system-level margin		20.0%	88.8
Total mass at launch			532.7
Soyuz Fregat 2-1b launch capacity[b]			620.0
Launch margin			87.4 (14.1%)

[a]To be detailed subsequently. [b]$C_3 = 38.84\ \mathrm{km^2 \cdot s^{-2}}$.

called the solar sail payload; however, the spacecraft will command and control the solar sail, which will not be capable of independent operation. The term spacecraft is, thus, more appropriate. The solar sail is a fully integrated subsystem of the spacecraft; however, for the purpose of technology definition requirements it is presented here as a separate entity.

Throughout the solar polar spacecraft design, full redundancy is maintained, except for the high-gain antenna (HGA). We note, further, that many components of the solar sail, such as sail film, cannot be supported through redundancy due to mass and/or volume considerations; however, full redundancy is applied to the sail where possible. The spacecraft systems analysis is based on a minimum solar approach thermal limit of 0.48 AU, the baseline mission profile. However, an analysis will also be presented as to the effect of varying the thermal limit. An overview of the spacecraft mass budget is shown in Table 1 as part of a complete launch mass breakdown. We note that the total spacecraft wet mass is 247.9 kg, of which 41.2 kg consists of the science instrument allocation. Table 1 gives the current best estimate (CBE) mass, which then has a design maturity margin (DMM) added to give the total subsystem mass allocation. The DMM is added at equipment level, where $>5\%$ is added for off-the-shelf items [European Cooperation for Space Standardisation (ECSS), category A/B], $>10\%$ for off-the-shelf items requiring minor modifications (ECSS category C), and $>20\%$ is added for new design/development items, or items requiring major modifications or redesign (ECSS category D). We note in Table 1 that the added DMM can appear somewhat arbitrary. For example, the power subsystem DMM is 8.3%. However, this is simply a result of averaging the DMMs allocated at the equipment level. We anticipate only limited technology issues with the spacecraft subsystems because the space environment at 0.48 AU is relatively benign in comparison with other currently envisaged missions, including BepiColombo[6] and the solar orbiter mission. Note, however, that direct adaptation of technology is rarely possible, and thus, some limited modifications and developments are inevitable.

Science Instruments

During this TRS, a representative set of instruments for the mission was defined, together with basic system-level requirements. Thus, a strawman payload was implemented to allow mission analysis. The current strawman payload comprises six instruments, detailed in Table 2. A relatively simple package of plasma instruments is required to relate the properties of the solar wind at 0.48 AU to the solar and coronal features studied with the remote sensing instruments. However, the spacecraft field must be low (preferably <1 nT), known, and constant so that the magnetometer data can be corrected

Table 2 Strawman payload budget

Component	CBE mass, kg	DMM, %	Total mass, kg	Average power, W
Coronagraph	10.0	10.0	11.0	10
Extreme ultraviolet imager	10.0	10.0	11.0	10
Velocity and magnetograph imager	10.0	15.0	11.5	10
Plasma analyzer	3.0	10.0	3.3	4
Magnetometer	2.0	10.0	2.2	4
Energetic particle telescope	2.0	10.0	2.2	4

onboard and used in reducing the plasma distributions from the three-dimensional measured distributions to the two-dimensional, field-aligned distributions to be returned to Earth. A deployable 2.5-m boom from the spacecraft was selected.

We recall the transfer trajectory mission phase lasts approximately 5 years. The mission can, thus, be significantly enhanced if the science suite can be utilized during this period, while the spacecraft retains the sail. Use of the science suite during the transfer trajectory would enable a full comparison of the solar environment at all latitudes. It is anticipated that the solar sail will have pointing accuracy of approximately 1 deg due to sail flexing, whereas pointing knowledge of the science suite would be high as this can be determined by the spacecraft's attitude and orbit control system (AOCS). Pointing stability of the science suite is difficult to determine, although we note that the lowest structural mode frequency of a solar sail is typically below 0.1 Hz (Refs. 7 and 8). Thus, it is feasible that while attached to the sail the pointing stability over very short integration times may be compatible with the required instrument stability, allowing some low-quality data to be generated by the imaging instruments during the transfer trajectory through the use of shortened integration times. Note, however, onboard autonomy would be required to select the images that are of scientific use because sail flexing means the instrument field-of-view may be suboptimally orientated. The pointing requirements of the plasma analyzer and magnetometer match the sail design specifications; however, it is unclear if the local spacecraft environment will be suitable for use of such instruments.[9] We note that the analysis within this paper assumes no science during the transfer trajectory.

AOCS

The AOCS is defined for the two distinct phases of being attached to the sail and then following sail jettison. The solar polar spacecraft is three-axis stabilized at all times, with a baseline pointing control of 360 arc-s following sail jettison provided for the payload instruments that are considered to be always on, such as the plasma analyzer and magnetometer. Higher, short-term pointing stability is provided for the imagers. It was found that little gain was made by relaxing the nominal pointing requirement because the magnetometer has a required pointing stability of 360 arc-s/s. Furthermore, maintaining pointing control at 360 arc-s allows the X-band HGA to be used at any time through the mission, for example, in space weather applications, with no impact on the AOCS hydrazine budget used for attitude control following sail jettison.

Pointing knowledge is maintained by a combination of coarse sun sensors, gyroscopes, and star sensors, while attached to the sail. Recall, the lowest structural mode frequency of a solar sail is typically below 0.1 Hz (Refs. 7 and 8); thus, because the sail flexes, the orientation of the thrust vector is fairly uncertain and highly accurate guidance becomes difficult, meaning that the sail will require many course corrections over the period of the transfer trajectory due to thrust vector misalignment errors. Pointing knowledge is maintained by star sensors and gyroscopes once the sail has been jettisoned and continuing through the science operations phase. Reaction wheels, which are unloaded through the use of a monopropellant system, maintain spacecraft pointing stability. It is not possible to use all instruments all of the time due to pointing requirements; however, we wish to maximize the use of all instruments. Analysis of propellant requirements leads to the conclusion that a hydrazine system is

preferable to a cold-gas system due to the reduction in propellant mass. We note that part of the AOCS propellant mass budget is a contingency propellant budget that is provided for use in the sail separation and avoidance maneuver, the specifics of which will be discussed later. The AOCS propulsion assumes a specific impulse of 200 s for pulse maneuvers and 230 s for longer duration burns, such as the sail separation and avoidance maneuver. The AOCS propellant mass total is 10.8 kg, as seen in Table 1.

Telemetry, Tracking, and Command

No significant technology requirements were identified within the telemetry, tracking, and command (TT&C) subsystem. However, some important trades were required to define an optimal solution between sail and spacecraft requirements that vary the system design from a nonsail delivered solar polar orbiter spacecraft.

Data latency is nominally set at less than 1 week, which coupled with a continuous science data acquisition stream of 3.5 kbps means that we acquire approximately 2.1 Gbit of data between downlinks. Assuming each downlink is 8 h, we can then define a required minimum science telemetry downlink rate of 73.5 kbps. Maximum slant range for the science operations mode is approximately 1.46 AU. At this slant range, we find that the required spacecraft transmitter power is just over 28 W. Therefore, to provide a margin for return of engineering data at all times, we set the spacecraft transmitter power at 30 W, giving a design telemetry rate (downlink) of 77.8 kbps and a command rate (uplink) of 38.9 kbps. The minimum margin for engineering data is 4.3 kbps; however, this margin increases to over 386 kbps at the minimum slant range of 0.6 AU.

As already discussed, the expected pointing accuracy while attached to the sail is low due to sail flexing, thus, limiting communications to X-band frequencies and lower while the spacecraft is attached to the sail. We can, however, consider adoption of a dual X and Ka-band system, which would allow increased data rates, reduced frequency of downlinks, and a reduction in power requirements during the science phase of the mission, or a combination of each. Using a 35-m dish in the Ka-band, at 20 kW to match ESA ground station network (ESTRACK) configuration, and increasing the spacecraft pointing accuracy during downlinks to 36 arc-s, as required for Ka-band, we can analyze such an option. AOCS mass marginally increases assuming one 1.5-m HGA downlink of 8 h per week in a 2-year mission due to the increased pointing requirements. The spacecraft transmitting power can be significantly decreased during the Ka-band HGA downlinks because the available command rate otherwise increases to over 8 Mbps and the telemetry rate to just less than 1 Mbps, assuming conditions such as antenna elevation and weather confidence are similar. However, to maintain sufficient link margins and data rates within the other communication modes, we require to maintain spacecraft transmitting power at 30 W within the X-band limited modes of cruise and emergency, negating the potential power saving available during the science operations mode. Furthermore, during the science operations mode the spacecraft is in a power-rich environment and, thus, power savings are not of significant benefit. We note, however, that adoption of Ka-band within the science operations mode would allow a solid-state power amplifier to be flown because spacecraft transmitting power requirements are only 5 W for one 8-h downlink per week, allowing increased subsystem reliability at the expense of additional mass. It is found that the adoption of a dual X and Ka-band communications architecture, with SSPA, increases the spacecraft total mass by 6.4 kg, which in turn increases sail side length by almost 2 m and total mass at launch by 11.9 kg. The selected spacecraft communications architecture is limited to X-band frequencies, which reduces HGA surface tolerance design limits and removes any potential requirement for a two-way capable Ka-band small deep-space transponder (SDST) because current SDST technology is limited to two-way X-band and downlink only in Ka-band.

Maintaining the spacecraft transmitting power at 30 W allows the calculation of the attainable data rates within the other communication modes. We see in Table 3 the available data rates in each communication mode, at the maximum design slant range. Each communication mode strives to minimize ground segment costs and requirements, hence, utilizing as small a ground station as possible, as detailed in Table 3. Note the design HGA size is 1.5-m diameter.

The use of alternative ground stations would clearly allow for increased data rates; however, sufficient data rates are attainable within each mode. It is considered optimal that data latency be set at the nominal value of 1 week, with a transmitter power rating of 30 W within all communication modes. Data can, however, be returned at increased frequencies, and so the data latency setting is a nominal design value that is used to define onboard memory requirements within the data handling subsystem.

The 0.48-AU orbit is not ideal for dedicated Earth-related space weather observations. However, the 0.48-AU orbit allows the observation of coronal mass ejections directed towards Earth for much of the time. The instrumentation onboard can, therefore, provide an additional contribution to space weather forecasts. The spacecraft could provide up to a 1-day warning of large solar proton events. The space weather communication architecture selected within this paper is based on beacon-mode technology. A simple tonal system is used to indicate whether or not an event has occurred. The beacon mode requires an onboard system that can communicate with Earth 24 h per day and at least three ground antenna, hence, the selection of ESTRACK 5-m stations as shown in Table 3, which are currently available and would require minimal further investment. Upon detection of an event, emergency use of a 35-m ESTRACK antenna commands the spacecraft to transmit a special downlink load. The additional cost and system requirements for operating the beacon mode are included in the baseline mission.

Power

The power subsystem analysis suggests no significant technology issues that we cannot reasonably expect to be solved within other currently active studies.[3,6] We note, however, that design techniques, such as advanced computer-aided design, allow the reduction of harness mass through better design methodologies; such mass savings are significant for enhancing solar sailing missions. The power system is supplemented by lithium ion batteries, which are designed to carry the power load during the launch phase and to absorb peak power loads during other mission phases, for example, during the transfer trajectory when sail pitch may limit array performance. The nominal power loads for solar array and battery sizing are defined in Table 4, where we see that the power load is split into three main categories. The design power load is defined as the nominal power load (Table 4) plus a 20% system-level margin. Solar array design is based on Spectrolab 26.8% improved triple junction solar cells.[10]

Table 3 Available data rates, at the maximum design slant range defined by trajectory analysis

Communication mode	Antenna–ground station, m	Mode design slant range, AU	Minimum data rate, kbps	
			Command	Telemetry
Cruise	LGA,[a] 15	1.80	0.03	0.04
Space weather	LGA,[a] 5	1.46	0.00	0.01
Science operations	HGA, 35	1.46	38.9	77.8
Emergency	LGA, 35	1.80	0.03	0.21

[a]Low gain antenna.

Table 4 Power budget

System	Launch power, design point 1 AU, W	Transfer power, design point 0.48 AU, W	Science power, design point 0.48 AU, W
Science instruments	0.0	0.0	24.7
AOCS	35.2	17.4	47.8
TT&C	0.0	73.9	73.9
OBDH	7.9	17.4	26.1
Thermal and radiation	83.1	83.6	83.6
Power	35.4	27.0	27.3
Mechanisms and structure	0.0	4.2	9.5
Solar sail	0.0	10.9	0.0
Nominal power load	161.6	234.4	292.9

To maintain the solar array within thermal bounds it is found that at end-of-life (EOL) the array must be pitched at over 63 deg from the sun line. However, the use of carbon–carbon substrates, as in BepiColombo, may also prove beneficial. The total array surface area is found to be 1.03 m^2, which is divided into two wings. The small surface area required allows for simple planar arrays to be envisaged, without the need for them to unfold following spacecraft launch. We note that despite the increased solar flux at 0.48 AU, the solar array design point was found to be at EOL due to array degradation during the mission, the significant thermal losses encountered at 0.48 AU, and that the power load is highest during this mission phase. The cell efficiency at EOL is 19%.

Remaining Spacecraft Subsystems

The onboard memory requirements are defined in part by the maximum data latency setting of 1 week; thus, the spacecraft acquires just over 2 Gbit of data between downlinks. Furthermore, it is required that the solar sail be highly autonomous, necessitating sizeable computational and storage capabilities.

Within the remaining subsystems, no significant technology issues were identified in this analysis. Note that the placement of the spacecraft within the plane of the sail film means that the heat generated by the sail, both reflected and emitted, has a very low view factor with respect to the spacecraft systems. Thus, the sail thermal input to the spacecraft is negligible. An initial radiation analysis suggested a conservative design tolerance of 75 krad should be adopted.

The spacecraft configuration is assumed to be a cube of sides 1.1 m. We note, however, from the solar orbiter mission studies that the spacecraft thermal design may be aided by adoption of a rectangular design rather than a cube. Figure 2 shows the SPO spacecraft in deployed configuration, allowing the volumetric requirements of the spacecraft to be analyzed and aiding in the launch vehicle configuration analysis later in this paper. The imaging science instruments are mounted internally, with field of view toward the sun along the negative X axis: This provides a clear field of view because the face is maintained in a sunward orientation through bias torque. A 2-axis steerable HGA is mounted on the anti-sun side, the positive X axis, and so the HGA is provided with a degree of thermal protection due to the shadow from the main spacecraft body. However, in this initial configuration, there is potential for the (hot) solar arrays to impinge the field of view of the HGA. Two sets of one-degree-of-freedom steerable solar arrays are mounted along the Z axis, either side of the main body of the spacecraft, allowing the solar aspect angle to be varied during the cruise phase of the mission while the spacecraft is attached to the solar sail. The solar arrays are small; thus, they are stowed against the $\pm Z$-axis faces during launch. The negative X axis, which faces the sun during the science phase of the mission, is provided with additional thermal protection. However, all spacecraft faces are required to have sufficient thermal control, because during the cruise phase of the mission the sail attitude may be such as to expose any spacecraft surface to the sun for a short period of time. The $-X$ face mounts the spacecraft onto the solar sail. By mounting the spacecraft via the $-X$ face, we shield the science instruments from the deep-space environment until after sail jettison, thus, helping to maintain optical surfaces in optimal condition. This configuration, however, eliminates the potential use of these instruments during the cruise phase of the mission.

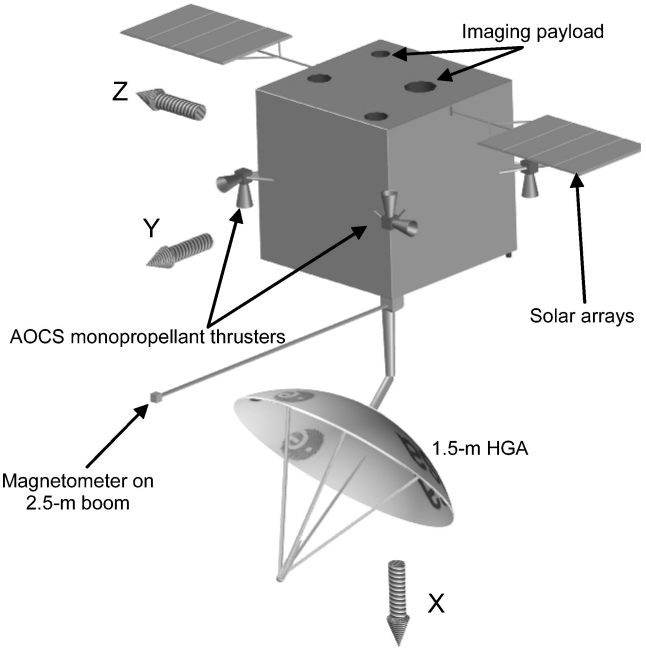

Fig. 2 SPO preliminary deployed visualization.

Variation of Minimum Solar Approach Radius

The spacecraft systems detailed earlier were designed for a minimum solar close approach of 0.48 AU. However, from a trajectory perspective, an optimal solution can be found by allowing closer solar approaches during transfer. As such, it is important to quantify the effect of varying the solar close approach radius on the spacecraft subsystems, to define this sensitivity. We see in Fig. 3 the effect of varying solar approach radius on the wet mass of the spacecraft, without the sail. The design points are intended to provide a good first approximation and as such are suitable for preliminary design analysis. The information in Fig. 3 will be coupled with trajectory and sail design information later in this paper to quantify fully the effect of varying the minimum solar approach radius.

Required Sail Slew Rates

From trajectory analysis, we note that inclination cranking constitutes the bulk of the transfer trajectory to the solar polar orbit. During the cranking phase, the sail pitch is fixed at $\arctan(1/\sqrt{2})$, while the sail clock angle flips from 0 to 180 deg (Ref. 11). However, it is clear that the sail thrust vector cannot be rotated through ~70.5 deg instantaneously. We, thus, investigate the effect of varying the sail slew rate to quantify requirements on the sail attitude control system. By examination of the locally optimal inclination control law[11] we anticipate that sail slew requirements should be rather low. The rate of change of inclination will approximate a signum function of a cosine curve, with the required sail slew maneuver naturally occurring when the rate of change of inclination is low.

Using a heliocentric trajectory model that includes orbit perturbations due to the terrestrial planets and that models the sun as a finite uniformly bright disk and the sail as an 85% efficient reflector, we propagate the orbit cranking sail trajectory for half an orbit revolution. We compare the inclination change over half an orbit against the instant sail slew scenario, allowing investigation of sail slew rates as seen in Fig. 4. Figure 4 shows the dropoff, or degradation, due to the finite sail slew rate on the rate of change of inclination. We see that at lower sail accelerations the degradation for a given slew rate is increased, whereas at lower solar radii the degradation is also increased due to the shortened orbit period. We see from Fig. 4 that above a sail slew rate of 10 deg/day (10^{-4} deg $\cdot$ s^{-1}) the degradation

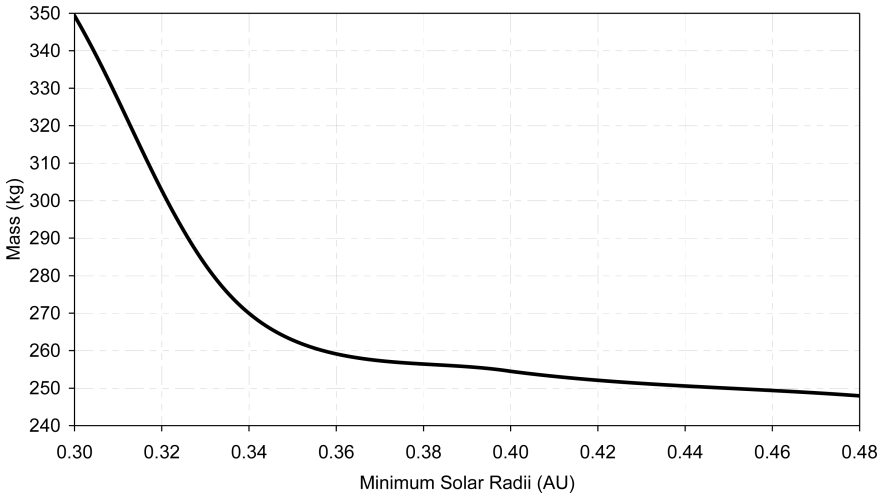

Fig. 3 Variation of total spacecraft mass as solar approach thermal limit is varied.

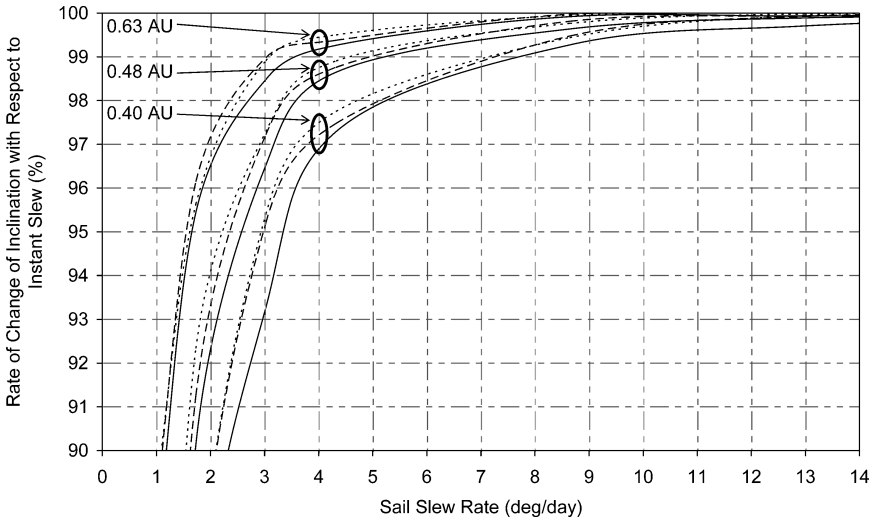

Fig. 4 Rate of change of inclination with respect to instant slew scenario; orbit radius indicated at top left, for three characteristic accelerations at each radius: ——, 0.4 mm · s^{-2}; – – –, 0.5 mm · s^{-2}; and · · · ·, 0.6 mm · s^{-2}.

of inclination change is less than 0.5% at all of the accelerations and solar radii considered. We, thus, define the required sail slew rate as 10 deg/day.

Sail Attitude Control

Prior solar sail attitude control system (ACS) studies are limited. Studies for the ST-7 sail estimated that a sail turn rate of 0.01 deg · s^{-1} was attainable,[7] significantly higher than the required value of $\sim 10^{-4}$ deg · s^{-1} for the SPO mission. The large moment of inertia of a solar sail and the low-frequency structural dynamics present many unique attitude control challenges. It has been determined that the solar sail required for the SPO mission need not be particularly agile; this significantly simplifies sail ACS hardware design. The optimal ACS solution will likely use the sail structure and mechanisms for attitude control rather than employ a secondary system, which would incur a mass penalty.[8]

Much prior sail design work has base-lined the use a deployable gimbaled boom due to the many apparently attractive features of such a design. However, it has become apparent on detailed study that such a solution is less than optimal due to a lack of full redundancy and control accuracy issues.[8] The use of tip vanes exclusively is also considered a suboptimal solution for a variety of reasons.[8] The optimal solution will, thus, likely employ a combination of systems, thus, the inclusion of a secondary system such as pulsed plasma thrusters should not be completely dismissed. In this paper, the use of sail tip vanes is assumed due to the lack of prior ACS studies. Thus, an appropriate mass allocation for the sail ACS is included within the sail design, while leaving open the potential for adoption of an alternative ACS.

Recall that the required time to slew $\sim$70.5 deg is approximately 7.05 days, averaging 10 deg/day. However, because the slew maneuver will be symmetrical about the zero clock direction, we can model the slew more accurately as acceleration through $\sim$35.2 deg followed by deceleration through $\sim$35.2 deg, each lasting $\sim$3.5 days. If the center of pressure and center of mass are perfectly aligned, we find that the sail can accelerate through $\sim$35.2 deg in $\sim$3.5 days with small tip vanes. It is, however, unlikely that the center of pressure and center of mass will be perfectly aligned due to deployment inaccuracies and sail flexing. Thus, we design the tip vanes to compensate for a given center of pressure and center of mass offset, as well as to be able to perform the required slew maneuver in the correct time. The tip vanes are assumed to be isosceles triangles because this minimizes the structural member mass assuming noninflatable technology is used.

Solar Sail Mass Budget and Definition

Recall from Table 1 that the total sail subsystems mass is 196 kg. The solar sail mass budget is detailed in Table 5, where it is seen that the mass of the four 14.9-m triangular tip vanes is 11.4 kg, giving a tip-vane assembly loading of 102.1 g · m^{-2}. We note that

the wires supplying power and command capability to the boom tips have a total mass of 12.7 kg and form a significant percentage of the total sail mass. Whereas the optimal ACS solution remains to be defined, the use of large tip vanes allows a suitable mass allocation to be defined, thus, leaving open the potential for adoption of an alternative ACS at some point in the future. The tip vanes are sized for a center of pressure/center of mass offset error of 0.25% the sail side length, which corresponds to 0.38 m for this design point. Prior solar sail studies for ST-7 also assumed a center of pressure/center of mass offset error of 0.25% (Ref. 7).

The square sail side length is 153 m, including a 10×10 m square central cutout to allow for sensor field-of-view requirements, at an assembly loading of 8 $g \cdot m^{-2}$. The main sail booms, which support the sail film, are based on a scaling from the Advanced CoilAble booms and a projected near-term solar sail technology roadmap.[12,13] It is seen in Table 5 that the sail stowage box mass allocation is split into several components, including primary and secondary structure, spacecraft adaptors, and sail deployment equipment. Note the sail stowage and deployment equipment is not jettisoned following sail deployment, as would be ideal. This apparent omission actually provides benefits for such an early mission and technology analysis by maintaining a conservative design ideology, which increases the sail technology demands above the apparent required level and allows for an increased technology margin. Furthermore, the actual method of jettisoning requires detailed study to ensure against sail film damage from jettisoned equipment. The spacecraft adaptor (carrier side) detailed in Table 5 provides the mass allocation of the sail jettison mechanism (SJM) on arrival at the target orbit. The mass allocation for the SJM is defined following launch vehicle adaptor methodologies,[14] due to the lack of current SJM designs. The SJM mass allocation is found as 5% of the spacecraft mass plus a 10% DMM. THE SJM mass is split 75:25 between the carrier, that is, the sail, and the spacecraft, respectively, thus minimizing spacecraft mass following sail jettison. The SJM, spacecraft side, is allocated within the mechanisms and structure subsystem and has mass of 3.4 kg. The second adaptor seen in Table 5 corresponds to the launch vehicle adaptor and is defined using criteria similar to the SJM.[14]

Table 5 Solar sail mass breakdown, with scaling laws rounded to one decimal place

Component	CBE mass, kg	DMM, %	Total mass, kg
2-μm CP-1 film substrate	66.4	20.0	79.6
0.1-μm Al sail front coating	6.3	5.0	6.6
0.01-μm Cr sail rear coating	1.7	5.0	1.7
Main sail bonding	1.9	10.0	2.0
Main sail booms (65.2 $g \cdot m^{-1}$)	28.1	20.0	33.8
Tip-vane mass	2.2	12.0	2.6
Tip-vane gimbal, motor, and housing	8.0	10.0	8.8
Tip-vane control wires	12.1	5.0	12.7
Sail stowage box			
Primary structure	19.4	10.0	21.3
Secondary structure	3.2	10.0	3.5
Deployment and auxiliary equipment	2.5	10.0	2.8
Spacecraft adaptor (carrier side)	9.3	10.0	10.2
Misc. apparatus, including deploy mechanisms	4.3	5.0	4.5
Launch adaptor (spacecraft side)	5.6	5.0	5.8
Total	170.7	10.3	195.9

The specifics of the solar sail deployment sequence and mechanisms are not defined within this paper because such detail requires specific hardware studies and trades to ensure the optimal sail deployment scenario is identified. The complete solar sail system requires significant further technology development.

Variation of Sail Systems Technology Parameters

The sail design specifications in Table 5 assume a 2-μm clear plastic-1 (CP-1) film substrate and main sail booms of specific mass 65.2 $g \cdot m^{-1}$. We can examine and quantify the effect of varying these parameters, allowing technology requirement specifications to be more accurately defined. We note that during this trade we fix the main boom specific mass at 50 $g \cdot m^{-1}$ when investigating sail film variations and fix the sail film as 2-μm CP-1 while examining main boom specific mass variations. All other parameters in Table 5 vary according to their relationship with the sail size, for example, as sail size increases the mass of sail film coatings will also increase.

The variation of boom specific mass linearly alters the sail size and mass. We note from the trajectory analysis later in this paper that the current launch C_3 sets a maximum launch mass of 620 kg, which corresponds to the minimum Soyuz Fregat 2-1b launch mass from Kourou. Increasing the boom specific mass to 150 $g \cdot m^{-1}$ we find that the total launch mass, including an ESA system-slevel margin of 20%, is 620 kg. Consequently, to maintain the current mission architecture and time line, for a 2-μm CP-1 film substrate, the maximum boom specific mass is 150 $g \cdot m^{-1}$, giving a sail size of 165 m.

The variation of sail film substrate material will have negligible impact on the sail system mass because most polyimide films have very similar densities. We, therefore, quantify the effect of varying substrate thickness for CP-1 film and polyethylene terephthalate (PET) film only because these two substrates represent the opposite ends of the spectrum. Note, however, that different polyimide films have significantly different thermal properties and as such can impact the allowed minimum solar close approach. We find that the use of 4-μm PET film results in a sail of side length 174 m, whereas the use of 5-μm CP-1 film results in a sail size of 198 m. Furthermore, we note that 1-μm film, such as a commercially available Mylar® film, would require a sail side length of only 140 m. Figure 5 shows

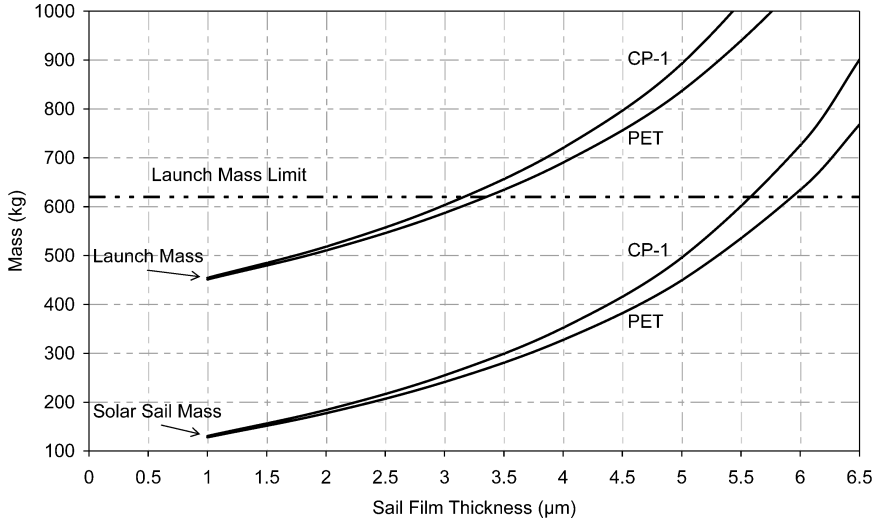

Fig. 5 Sail film substrate thickness variation vs sail mass and total launch mass.

the effect on sail mass and launch mass as sail substrate thickness is increased. We note that with an upper launch mass limit of 620 kg we can define the required sail film thickness as 3.2–3.4 μm, depending on film material, for a boom specific mass of 50 $g \cdot m^{-1}$. Recall that a boom specific mass of 65 $g \cdot m^{-1}$ is ultimately selected along with 2-μm CP-1 film.

Sail/Spacecraft Separation

Following arrival at the 0.48 AU polar orbit, we require a sail separation maneuver before initiation of the science phase of the mission. The AOCS propellant budget contains 2.2 kg of hydrazine specifically for sail separation and avoidance maneuvers. On separation from the spacecraft, the sail characteristic acceleration increases to 0.98 $mm \cdot s^{-2}$ due to the reduction in nonreflective mass. Modeling the separate sail and spacecraft trajectories, we find that the separation distance increases at approximately 1 km/min, assuming that no propulsive burn is performed by the spacecraft and that the sail remains passively stable at a setting of zero pitch to the sun. It is, thus, possible that the spacecraft may not require the use of its separation and avoidance propellant contingency initially to separate from the sail. However, if we continue to propagate the two trajectories, we find that the sail and spacecraft would go by within 100 km of each other when they both pass over the northern ecliptic pole for the first time, again assuming the sail remains passively stable at a setting of zero pitch to the sun. It is, however, likely that the sail will begin to tumble sometime after separation from the spacecraft because it is now uncontrolled. These initial calculations, thus, suggest that the spacecraft may only require the use of its separation and avoidance propellant contingency to perform sail avoidance maneuvers once the sail begins to tumble but not immediately following sail separation. Because sail separation is clearly a key technology issue, these initial findings must be further challenged and should be demonstrated in early sail technology demonstration missions.

Launch Configuration and Visualization

Assuming a 2-μm CP-1 film sail substrate and 65-$g \cdot m^{-1}$ main sail booms, we can investigate the launch configuration and investigate launch fairing compatibility with the Soyuz Fregat 2-1b vehicle. Figure 6 shows that significant volume is available for systems growth and no launch fairing compatibility issues are anticipated. Figure 6 shows the SPO spacecraft on top of the sail deployment box, with the sail booms shown in their stowed configuration. The main sail booms stow to between 1 and 2% of their deployed length.[12] The sail film is stowed within the central compartment of the deployment box, revealed only after boom deployment.

Trajectory Analysis

We recall that the target solar polar orbit is defined as inclined at 82.75 deg with a right ascension of 255.8 deg plus 0.014 deg/year from J2000, within a standard ecliptic plane reference frame. Furthermore, it is desirable that the polar orbit be correctly phased with the Earth to aid mission science returns and avoid solar conjunctions.

Transfers to solar polar orbits have been analyzed in parametric studies by Sauer[15] and briefly by Leipold.[16] After a short optimized spiral to a zero- or low-inclination circular orbit at the defined minimum solar approach radius, an analytical control law that maximizes the instantaneous rate of change of inclination is used to increase orbit inclination rapidly.[11] Following Sauer,[15] we have adopted a multiphase approach to the trajectory structure. Closer cranking orbit radii enable more rapid acquisition of polar inclinations, and a third outward spiral phase may be necessary to reach the first few resonant orbits, specifically, $N = 1$, 2, and 3.

The variational equations of the modified equinoctial orbital elements are explicitly integrated using an adaptive step-size, variable-order, Adams–Moulton–Bashforth method. The thrust vector direction has been defined by two angles to cover completely the outward hemisphere of allowable orientations. These are the pitch angle, $\alpha \in [0, \pi/2]$, between the sail normal and the sun line and the clock angle, $\delta \in [0, 2\pi]$, between the projection of the sail normal and a reference direction onto a plane normal to the sun line. A direct, parameter optimization scheme was implemented with the controls specified at discrete nodes at the segment boundaries, equally spaced in time between zero and the terminal time. The controls were characterized across each time segment by linear interpolation between the nodes. As the number of nodes was increased, then a close approximation to a continuous profile was achieved. Problems requiring more revolutions, or more rapid control variation (usually for lower accelerations), clearly needed more segments. To represent the optimized trajectories, in this paper, 50 segments (51 nodes)

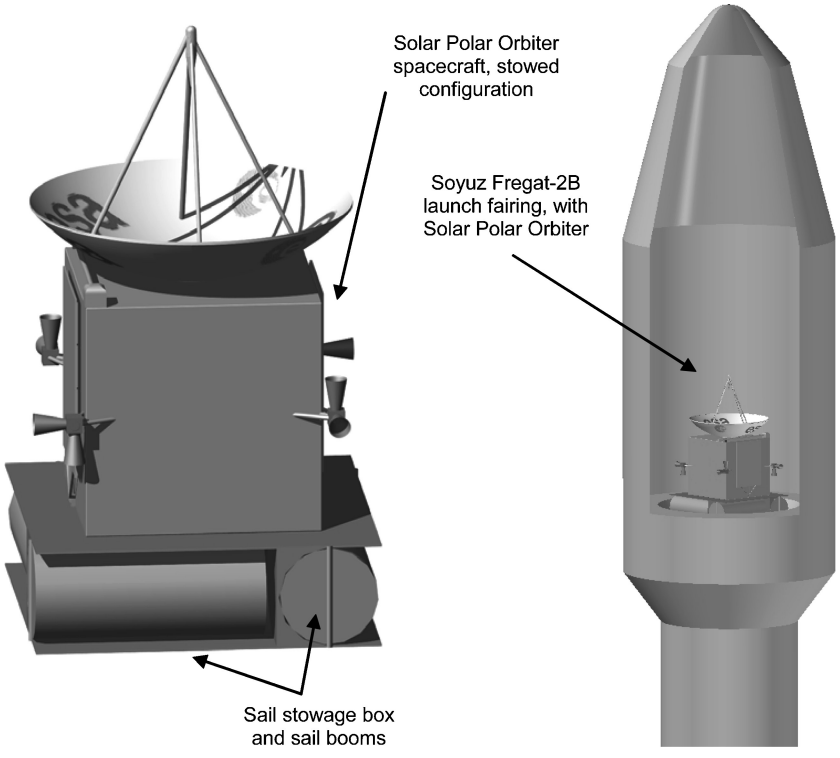

Fig. 6 Launch configuration and visualization.

were considered sufficiently accurate. The trajectory optimization problem is to select the variables that minimize the transfer time (objective function) while satisfying the endpoint boundary conditions (constraints). This was transcribed to a nonlinear programming problem, solved using NPSOL 5.0, a FORTRAN77 package based on sequential quadratic programming (SQP).[17] SQP employs a quasi-Newton approximation to the Karush–Kuhn–Tucker conditions of optimality, resulting in a subproblem of minimizing a quadratic approximation to the function of Lagrange multipliers incorporating the objective and constraints. Optimality termination tolerance was set to 2×10^{-4}, with the constraint feasibility tolerance at 6.69×10^{-6}. This ensured that final boundary conditions were satisfied to within 1000 km for each position element and to within 0.2 $m \cdot s^{-1}$ for each velocity element without performing excessive iterations. NPSOL is a gradient-based, deterministic, local search procedure and, therefore, requires an initial guess for the cone and clock angle profiles and transfer time that is within the proximity of the actual solution, ensuring a feasible solution is obtained. This was established using homotopy methods to map the initial guess to the final answer.[18]

Approximate Trip Times

Initial, approximate trip times can be obtained by adding the trip times for each of the phases. This, however, neglects the phasing of the orbits, the Earth ephemeris, and the orientation of the line of nodes of the polar orbit. Note that the line of nodes requirement means that a minimum trip-time opportunity occurs every six months. The launch window can, however, be considered open at all times through the year, with a trip-time penalty incurred as launch varies from the two optimal start epochs. In general, the actual trip time will be slightly longer than these approximate times, as will be seen later.

It is seen in Fig. 7 that the cranking time is very sensitive to the cranking orbit radius, although the curve levels off at higher accelerations. The closer the orbit is to the sun, the faster the inclination changes. The rate of change of inclination is, however, constant per integer number of orbit revolutions and is independent of orbit radius, assuming a circular orbit.[11] Low-radius orbits have shorter periods, and so the inclination change is effected more rapidly. For a launch C_3 of zero, optimizing circular-coplanar transfers from 1 AU to the polar/cranking orbit radius using NPSOL produced inward spiral trip times. The spiral times were added to the cranking times at the resonant orbit radii and the total two-phase trip time was found. Cranking at 1 or 0.63 AU is tremendously time consuming; thus, a three-phase approach must be adopted to reach these orbits. Furthermore, a three-phase approach is beneficial for the higher resonance numbers if the close solar orbit thermal loads can be withstood, as seen in Fig. 7. Figure 7 concurs with the 0.5-mm $\cdot s^{-2}$, two-phase transfer to 0.48-AU polar orbit that was previously generated and found to have a duration of order 5 years.[4,15] Note here that past work does not include positive C_3 launches or take into account Earth ephemeris, orbital orientation, and phasing, which will be included later in this paper. A moderate characteristic acceleration of 0.5 mm $\cdot s^{-2}$ would require a close cranking orbit of 0.3 AU for a mission duration below 5 years to a $N = 1$ orbit. Using a positive launch C_3 could alleviate this requirement.

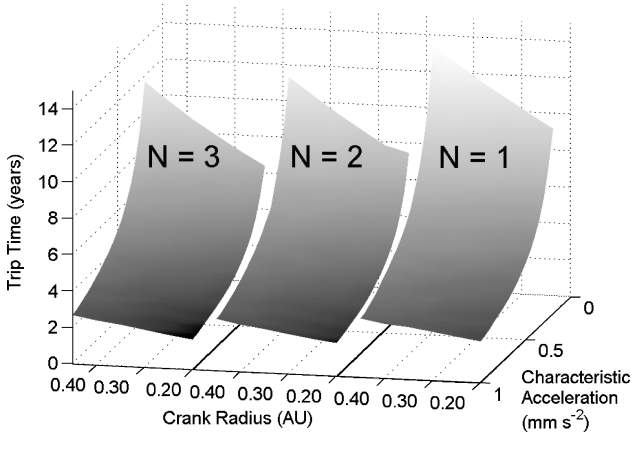

Fig. 7 Three-phase total trip times to $N = 1$, 2, and 3 solar polar orbits.

Optimized Inward Spirals to Circular Low Inclination Orbits at 0.48 AU

In the parametric study conducted by Sauer,[15] the inward spiral is optimized to 15-deg inclination before starting the cranking maneuver. If a third outward spiral phase was required, then the final 15 deg to reach polar orbit was also optimized. Sauer uses a locally optimal inclination control law, which has the drawback of making the generation of fully phased orbits very difficult. It was also noted that the total transfer time is relatively insensitive to initial cranking orbit inclinations above 10 deg (Ref. 15). This paper concentrates on the two-phase transfer to a 0.48-AU polar orbit. The effect of optimizing a circle-to-circle inward spiral from 1 to 0.48 AU was investigated, for a number of different target orbit inclinations. The optimized inward spiral times were added to the remaining cranking time necessary to match the inclination to polar orbit. The NPSOL optimization matched the semimajor axis, eccentricity, and inclination as constraints. It was found that, although the overall saving is less than 6 months, optimizing to 10–20 deg is significantly better than for 5 deg. In general, 15 deg seems the optimum value, as was found by Sauer.[15] As the initial cranking orbit inclination is increased beyond these values, many more revolutions are needed, and so the optimizer requires more control nodes, placing greater demands on the optimizer.

Utilizing Excess Launch Energy

Circular-coplanar optimizations of the inward spiral phase were conducted while increasing the launch C_3 to 40 $km^2 \cdot s^{-2}$, in opposition to the velocity of the Earth. We note that nonzero launch declinations were found to have a significantly adverse effect on sail transfer times and are, thus, not utilized. There were 51 control nodes used. Figure 8 shows the effect of using positive C_3 on the spiraldown time to a 0.48-AU circular orbit over a range of characteristic accelerations. For higher accelerations and higher cranking orbit radii, it was found that the curve levels off sooner than for low accelerations and low cranking orbits. There is, therefore, an increased benefit in using the excess C_3 capability to reach lower cranking orbit radii with low-performance sails.

We recall that a characteristic acceleration of 0.5 mm $\cdot s^{-2}$ was designated earlier within the approximate analysis to reach a 0.48-AU polar orbit with a total transfer time of order 5 years. An attempt was made to reduce the sail performance requirements by using the excess C_3 available, with optimized spiralin to 15–20 deg inclination. To produce an approximate SPO transfer with a trip time of order 5 years, it was found that the characteristic acceleration needed was of order 0.42 mm $\cdot s^{-2}$ for a C_3 of 40 $km^2 \cdot s^{-2}$. We note that the Soyuz Fregat 2-1b from Kourou has a minimum launch mass of 620 kg, corresponding to a zero declination positive C_3 of 38.8 $km^2 \cdot s^{-2}$; thus, we anticipate that the actual trip time will be slightly in excess of 5 years.

Gravity Assist Option

It is now considered whether any significant benefit can be obtained for the mission from unpowered gravity assists. Multiple gravity assists within the inner solar system tend to be prolonged in duration and can be limited in launch window frequency, especially if considering nonresonant combinations. We, therefore, anticipate that any benefit will occur through use of a single gravity assist maneuver, probably at Venus, because this will allow for a perihelion inside the Venusian orbit. Use of a Mars or Earth flyby would result in a high aphelion, which is detrimental to solar sailing. Furthermore, it is envisaged that sail deployment will commence only after the final gravity assist, due to navigational difficulties with such a large structure and inaccurate pointing control due to sail flexing. The delayed deployment of the sail will avoid the need for accurate sail navigation and control during the gravity assist, but would require some additional propellant on the spacecraft bus for trajectory

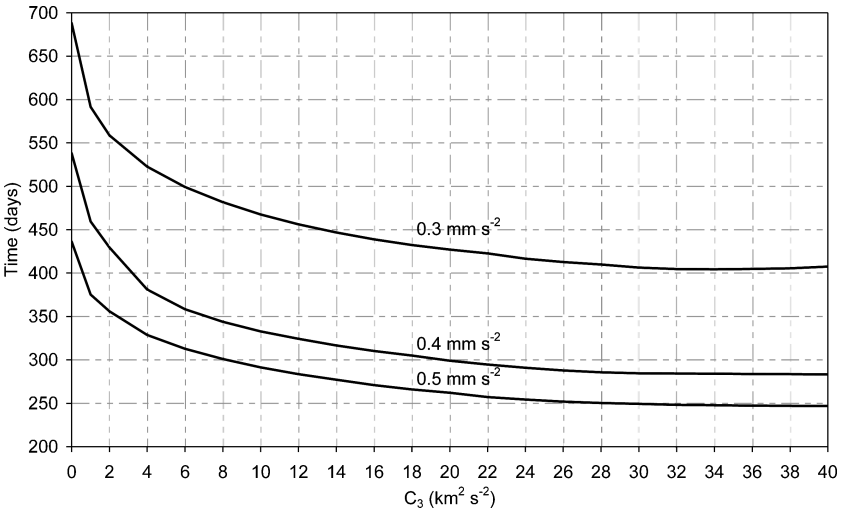

Fig. 8 Spiralin time to circular cranking orbit at a radius of 0.48 AU for characteristic accelerations of 0.3, 0.4, and 0.5 mm · s^{-2}, against launch C_3.

correction maneuvers, probably within the AOCS hydrazine budget. Furthermore, the significant level of available launch C_3 means that sail deployment before a Venus flyby would have negligible impact on the duration of this transfer.

Launching on 27 December 2017, we perform a 2883-km Venus flyby 142 days later on 18 May 2017, placing the undeployed solar sail on a 0.73 AU × 0.52 AU × 18 deg orbit. After sail deployment, on this orbit the primary trajectory goal is to circularize the orbit at 0.48 AU. During orbit circularization, it was found that the orbit inclination can be increased slightly with no degradation on the circularization goal, so that the sail arrives on an orbit of 0.48 AU × 0.48 AU × 22.32 deg after 195 days, 337 days after launch. Note that this trajectory analysis was performed using A^{n}D blending, a method that blends locally optimal control laws and allows a more rapid analysis than traditional methods.[19–22] Each control law is prioritized by consideration of how efficiently it will use the solar radiation pressure and how far each orbital element is from its target value. It has been demonstrated that trajectories found with A^{n}D blending are very similar or better than those found using traditional trajectory optimization methods.[21,22] On arrival at the circular 0.48-AU orbit, the locally optimal inclination control law is once again used to raise the orbit inclination. The complete orbit transfer duration is 4.13 years from the Venus flyby, giving a total flight time from launch of 4.52 years. An unpowered Venus gravity assist can, thus, provide a saving of 0.4 years for a reduced sail acceleration of 0.4 mm · s^{-2}. Thus, the use of a Venus gravity assist can, as anticipated, offer some potential benefits over a conventional mission profile, although the saving in transfer time and sail performance appear modest. This option was not selected as the reference trajectory because at this stage of analysis it was felt a conservative estimate of solar sail technology requirements was required. Moreover, the technological challenge of stowing a sail for approximately 150 days in the space environment before an autonomous deployment at 0.6-AU slant range was considered significant. Furthermore, it was considered problematical to emulate in a technology demonstration mission to reduce the risk. Note that the slight reduction in sail size would be somewhat offset by the increase in required spacecraft mass due to the increase in propellant mass; this was not modeled here. Note, however, that a Venus gravity assist provides some benefit and, thus, remains a valid option during future analysis.

Fast Mission Option

An alternative mission option would be to employ a three-phase strategy, to reach a 0.48-AU polar orbit more rapidly. The cranking orbit was set at 0.30 AU, with the minimum solar radius also constrained at this distance. A slight increase in the characteristic acceleration to 0.5 mm · s^{-2}, with an increase in the mass of the thermal subsystem, means the sail side length is of order 200 m. The increased launch mass results in a maximum available C_3 of 27.9 km^2 · s^{-2}. The optimized, positive C_3 inward spiral time (coplanar) was found to be 320 days. The orbit then cranks up to 82.75 deg in 706 days. The third phase was then optimized to spiral outward from the cranking orbit to the final orbit radius of 0.48 AU, in 110 days. The total trip time to polar orbit was 3.11 years, for this fast-mission option; however, savings could be made by removing the coplanar transfers. Figure 9 shows the entire three phases of the trajectory. Although this option offers a significant time saving, the increased risk and cost of a prolonged stay at 0.3 AU, coupled with the increase in sail size, meant this option was considered suboptimal.

Reference Trajectory

The problem of obtaining the correct phasing at arrival on the solar polar orbit was deemed to be best tackled by selecting an arrival date and position on the solar polar orbit that is correctly phased with the Earth. Then the analytical cranking control law was used to propagate the trajectory over a negative time span, thus, reducing inclination. The resultant orbital elements were then used as the initial conditions for a further reverse optimization, back to Earth. Integration over a negative time span has been used for low-thrust trajectory optimization in the past, for example, the early SMART-1 mission studies[23]; however, it has not previously been used to generate correctly phased solar polar orbits. The arrival position was selected as the north solar pole, with the Earth–sun–sail angle at 90 deg. The Earth was found to be at this azimuth angle in the early hours of 7 June 2015 (universal time), which was, thus, defined to be the SPO arrival date, allowing for an approximate Earth departure date in 2010.

For a characteristic acceleration of 0.42 mm · s^{-2}, the spacecraft is launched on 16 May 2010, with a positive launch excess energy of $C_3 = 38.84$ km^2 · s^{-2}, the maximum available from a Soyuz Fregat 2-1b from Kourou. A constraint was placed on the minimum solar radius of 0.48 AU. The optimal sail spiraldown to the cranking orbit is inclined to 14.42 deg in 457.5 days. This intermediate orbit has a semimajor axis of 0.4828 AU and an eccentricity of 0.0762 AU. The analytical cranking then takes place from 17 August 2011, raising the inclination to 82.75 deg at a circular 0.48-AU solar polar orbit in 1390 days. The complete trajectory is shown in Fig. 10, where the total transfer duration is 5.06 years. The maximum Earth–spacecraft distance is 1.654 AU, which is well within the maximum cruise mode slant range of the TT&C system, Table 3.

On arrival at the target orbit, the sail is jettisoned as discussed earlier. A high-fidelity trajectory model was used to propagate the solar polar orbit over 2 years with perturbations from the all of the planets out to and including Saturn. As expected, the orbital elements deviate by a negligible amount from the nominal values, with the

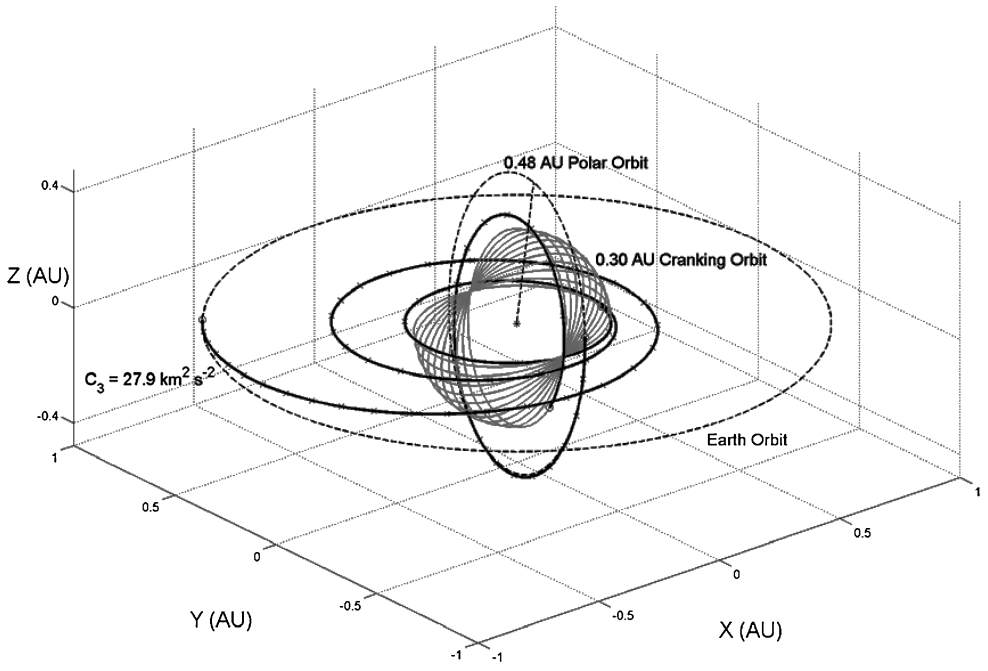

Fig. 9 Fast mission, $0.5 \cdot$ mm s^{-2} solar polar orbit trajectory.

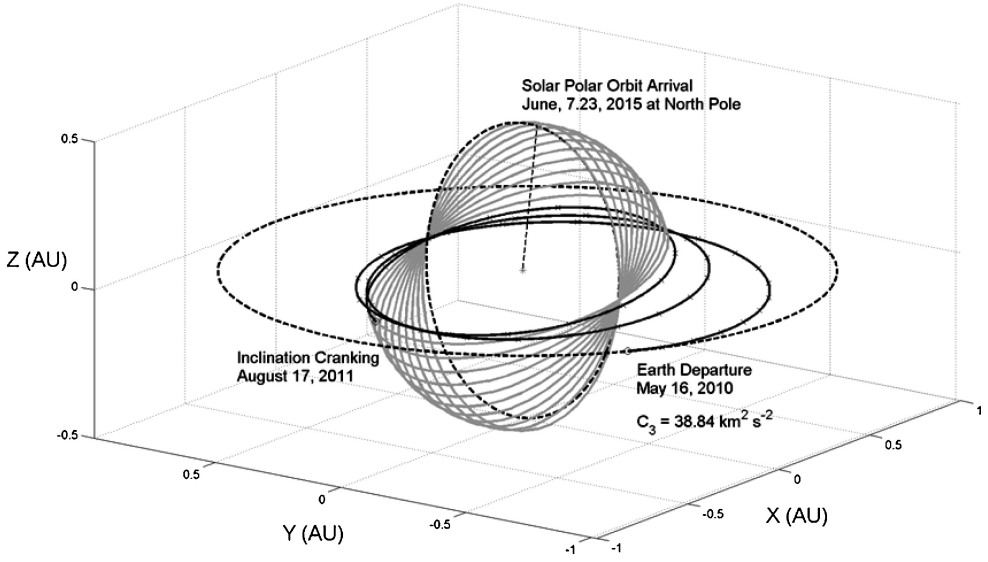

Fig. 10 Reference mission, $0.42 \cdot$ mm s^{-2}, solar polar orbit trajectory.

maximum Earth–spacecraft distance found to be 1.45 AU, which is within the maximum science mode and space weather mode slant ranges of the TT&C system (Table 3).

Competing Propulsion Options

The delivery of a spacecraft into a solar polar orbit is a challenging mission concept, as has been seen by the inability of the solar orbiter mission to attain a solar polar orbit with current SEP technology.[3] The velocity change requirement to attain a solar polar orbit with chemical propulsion is of order 42–56 km $\cdot$ s^{-1}, depending on N. Thus, chemical propulsion alone cannot provide a solar polar orbit, and we must consider the use of gravity assist maneuvers. To reach an aphelion within the Earth's orbit, we must restrict flybys to the terrestrial planets. However, the small mass of these planets means that the time to a polar orbit is unrealistically high.

The elimination of both conventional SEP and chemical propulsion as competing systems restricts our analysis to new and novel propulsion systems, such as nuclear electric propulsion (NEP), radioisotope electric propulsion (REP), or minimagnetospheric plasma propulsion (M2P2). It is expected that any NEP system will require a large launch vehicle due to the inherent nature of the system, thus, eliminating the use of a Soyuz-Fregat vehicle. Meanwhile, the use of a REP system would require extremely advanced radioisotope power sources to compete with solar power. For example, if we replace the solar arrays with an advanced radioisotope power systems of the same mass, we would require a power density of 13.5 W $\cdot$ kg^{-1}. However, if we add in a 5-kW electric propulsion system, the solar array mass rises to just under 80 kg, for a total array surface area of 20 m^2, which would require an ARPS specific mass of over 50 W $\cdot$ kg^{-1} to match the power mass budgets. M2P2 could potentially provide the required change in velocity needed to attain a true solar polar orbit. This concept is akin to solar sails, but has the advantage of not requiring large structures to be deployed. The drawback to this propulsion method is that the magnetic field generating system mass may be quite high. The lack of viable competing propulsion systems serves to highlight the potential of solar sailing for a solar polar mission concept. We, thus, conclude that solar sailing offers great potential for this mission concept and indeed

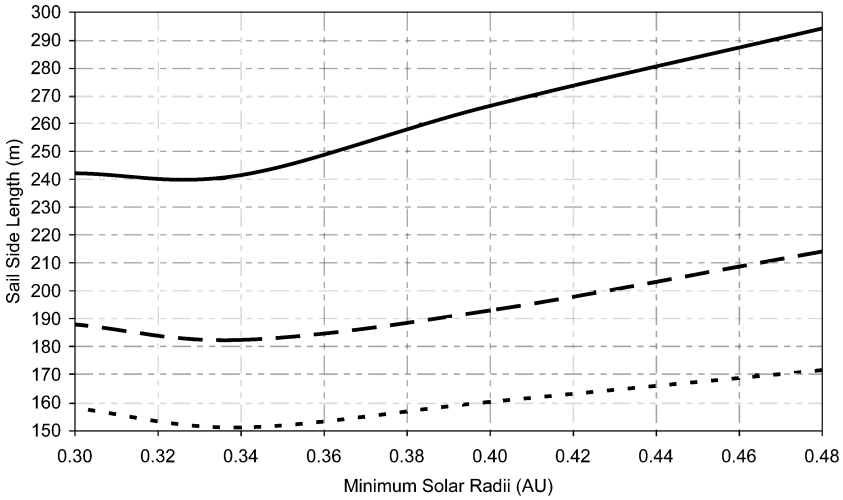

Fig. 11 Minimum solar radius vs sail size: – – –, 5-year; — —, 4-year; and ——, 3-year trip times to 0.48-AU solar polar orbit.

may represent the first useful deep-space application of solar sail propulsion.

Variation of Minimum Solar Approach Radius

We see from Figs. 3 and 7 the effect of varying the minimum solar approach radius on spacecraft mass and transfer duration to the polar orbit. Using the extensive parametric trajectory data set generated, we can estimate sail characteristic acceleration requirements for a given minimum solar approach radius and trip time to the 0.48-AU solar polar orbit, for a launch C_3 of zero. Thus, by combining sail characteristic acceleration requirements, spacecraft mass, and minimum solar approach radius we can quantify the global effect of varying the minimum solar approach radius. During this trade, we assume 2-μm CP-1 sail film substrate and 50-g $\cdot$ m^{-1} main sail booms, along with the sail design scaling discussed earlier and the spacecraft masses in Fig. 3.

Figure 11 shows the effect of varying the minimum solar approach radius on sail side length. We note that, despite the significantly increased spacecraft mass required to survive such a severe thermal environment, a minimum sail side length occurs for a minimum solar approach radius of 0.33–0.34 AU depending on desired mission transfer duration. A 5-year transfer trajectory can, thus, be attained with a sail of side length 150 m and minimum solar approach radius 0.34 AU. A similar trade was performed for launch mass vs minimum solar approach radius. It was found that the minimum launch mass varied from 0.34 to 0.36 AU, for trip time of 3–5 years, respectively. Thus, the minimum sail size does not provide for a minimum launch mass. However, the launch mass of the minimum sail size configuration for a 5-year transfer was less than 620 kg, the lower bound limit of the Soyuz Fregat 2-1b from Kourou, and as such, optimizing the launch mass can be considered secondary to sail size optimization. The use of a positive launch energy in this paper allows for a reduction in sail size toward the same value as an optimal (minimum sail size) architecture $C_3 = 0$ launch.

Conclusions

An SPO mission concept has been presented as a TRS. The mission utilizes a Soyuz Fregat 2-1b launched from Kourou. The low launch mass of 532 kg, including margins, allows for maximum launch energy to be used, providing the sail with an initial Earth C_3 in excess of 38 km$^2 \cdot$ s^{-2}. The use of positive C_3 and a single Venus flyby were shown to reduce the sail performance requirements, though the later was not adopted. The mission primary propulsion system was defined a priori as solar sailing, and we find that the required sail is 153 $\times$ 153 m for the baseline 5-year transfer mission scenario. However, sail size can be reduced through closer solar approaches despite the significantly increased spacecraft mass required to survive the increasingly hostile environment at low solar radii. Optimal close approach radii were presented to minimize launch mass and sail size, all of which were above 0.3 AU. A comprehensive trajectory study was completed, and for the first time, a trajectory was generated to an accurately phased and positioned orbit.

The solar sail and spacecraft technology requirements have been addressed. The sail requires advanced boom and new thin-film technology. The sail was found to be at a low-technology readiness level requiring significant further effort. By contrast, the spacecraft requirements were found to be minimal because the spacecraft environment is relatively benign in comparison with other currently envisaged missions. However, the spacecraft design was found to vary in some key areas from a nonsail delivered mission due to, for example, sail pointing accuracy limiting the communications system to X-band and below. Overall, the technology requirements for an SPO mission have been clearly identified.

Acknowledgments

This study was conducted under Contract European Space Research and Technology Centre 16534/02/NL/NR: Technical Assistance in the Study of Science Payloads Transported Through Solar Sailing. The authors thank Henry Garrett of the NASA Jet Propulsion Laboratory for his input into the study of potential cruise phase science issues regarding sail interactions with the space environment.

References

[1]Lyngvi, A., Flakner, P., Renton, D., van der Berg, M. L., and Peacock, A., "Technology Reference Studies," Electronic Proceedings of 55th International Astronautical Congress, Paper IAC-04-U.1.06, Oct. 2004.

[2]"Ulysses," ESA Science and Technology, URL: http://sci.esa.int/science-e/www/area/index.cfm?fareaid=11 [cited 12 June 2004].

[3]"Solar Orbiter," ESA Science and Technology, URL: http://sci.esa.int/science-e/www/area/index.cfm?fareaid=45 [citied 12 June 2004].

[4]Goldstein, B., Buffington, A., Cummings, A. C., Fisher, R., Jackson, B. V., Liewer, P. C., Mewaldt, R. A., and Neugebauer, M., "A Solar Polar Sail Mission: Report of a Study to Put a Scientific Spacecraft in a Circular Polar Orbit About the Sun," *SPIE International Symposium on Optical Science, Engineering and Instrumentation*, July 1998.

[5]Balthasar, H., Stark, D., and Wöhl, "The Solar Rotation Elements i and Ω Derived from Recurrent Single Sunspots," *Astronomy and Astrophysics*, Vol. 174, 1987, pp. 359, 360.

[6]"BepiColombo," ESA Science and Technology, URL: http://sci.esa.int/science-e/www/area/index.cfm?fareaid=30 [cited 12 June 2004].

[7]Wie, B., "Sail Flatness, Attitude, and Orbit Control Issues for an ST-7 Solar Sail Spacecraft," NASA SSTWG FY01, Solar Sail Technical Interchange Meeting, NASA Goddard Space Flight Center, 2001.

[8]Murphy, D., and Wie, B., "Robust Thrust Control Authority for a Scalable Sailcraft," American Astronautical Society, Paper AAS 04-285, 2004.

[9]Garrett, H., Wang, J., "Simulations of Solar Wind Plasma Flow Around A Simple Solar Sail," *Proceedings of the 8th Spacecraft Charging Technology Conference*, edited by R. Suggs, 2003.

[10]Spectrolab Photovoltaic Data Sheet, www.spectrolab.com [cited 12 June 2004].

[11]McInnes, C. R., *Solar Sailing: Technology, Dynamics and Mission Applications*, Springer-Praxis, Chichester, England, U.K., 1999.

[12]Murphy, D. M., and Murphey, T. W., "Scalable Solar-Sail Subsystem Design Concept," *Journal of Spacecraft and Rockets*, Vol. 40, No. 4, 2003, pp. 539–547.

[13]Macdonald, M., and McInnes, C. R., "A Near-Term Roadmap for Solar Sailing," Electronic Proceedings of 55th International Astronautical Congress, Paper IAC-04-U.1.09, Oct. 2004.

[14]Wertz, J. R., and Larson, W. J. (eds.), *Space Mission Analysis and Design*, Kluwer Academic, Dordrecht, The Netherlands, 1999, Sec. 11.6, pp. 459–497.

[15]Sauer, C. G., Jr., "Solar Polar Trajectories for Solar-Polar and Interstellar Probe Missions," American Astronautical Society, Paper AAS 99-336, Aug. 1999.

[16]Leipold, M., "Solar Sail Mission Design," Ph.D. Dissertation, DLR German Aerospace Center, Cologne, Germany, Feb. 2000.

[17]Hughes, G. W., McInnes, C. R., "Small Body Encounters Using Solar Sail Propulsion," *Journal of Spacecraft and Rockets*, Vol. 41, No. 1, 2004 pp. 140–150.

[18]Hughes, G. W., "A Realistic, Parametric Compilation of Optimised Heliocentric Solar Sail Trajectories," Ph.D. Dissertation, Dept. of Aerospace Engineering, Univ. of Glasgow, Glasgow, Scotland, U.K., June 2005.

[19]Macdonald, M., and McInnes, C. R., "Realistic Earth Escape Strategies for Solar Sailing," *Journal of Guidance, Control, and Dynamics*, Vol. 28, No. 2, 2005, pp. 315–323.

[20]Macdonald, M., and McInnes, C. R., "Analytical Control Laws for Planet-Centered Solar Sailing," *Journal of Guidance, Control, and Dynamics*, Vol. 28, No. 5, 2005, pp. 1038–1048.

[21]Macdonald, M., McInnes, C. R., and Dachwald, B., "Analytical Control Laws for Heliocentric Solar Sail Orbit Transfers," *Journal of Spacecraft and Rockets* (submitted for publication).

[22]Macdonald, M., "Analytical Methodologies for Solar Sail Trajectory Design," Ph.D. Dissertation, Dept. of Aerospace Engineering, Univ. of Glasgow, Glasgow, Scotland, U.K., May 2005.

[23]Schoenmaekers, J., Pulido, J., and Jehn, R., "SMART-1 Mission Analysis: Moon Option," ESA, Rept. S1-ESC-RP-5001, No. 1, Noordwijk, The Netherlands, Sept. 1998.

C. Kluever
Associate Editor